



Development and Cyclic Behavior of U-Shaped Steel Dampers with Perforated and Nonparallel Arm Configurations

Kurtulus Atasever¹ · Oguz C. Celik² · Ercan Yuksel³

Received: 13 February 2018 / Accepted: 2 May 2018 / Published online: 30 May 2018
© Korean Society of Steel Construction 2018

Abstract

Metallic dampers are sacrificial devices (fuses) that dissipate significant energy during earthquakes while protecting other parts of structures from possible damage. In addition to numerous implementation opportunities of other base isolation systems, U-shaped dampers (UD) are one of the widely investigated and used devices in practice especially in Japan. The present study focuses on enhancing seismic performance of these types of dampers by changing their geometric properties. UDs with perforated (i.e. with holes) and/or nonparallel arms are developed for this purpose. For a better comparison, the criterion of equal material volume (or mass) has been utilized. Three dimensional finite element models of the new type of UDs are formed and investigated numerically under selected displacement histories. Based on the obtained hysteretic curves; dissipated energy intensities, effective stiffness ratios, reaction forces, effective damping ratios are evaluated in this parametric study. It is found that both damper types have merits in use of seismic applications and that the selection of the damper configuration is dependent on the design specific issues.

Keywords Seismic isolation · Metallic dampers · Hysteretic behavior · Finite element analysis

1 Introduction

Seismic energy dissipation through large inelastic deformations of metallic dampers is one of the cost effective solutions among the existing seismic protection systems. Many past studies have focused on the behavior of structures (both buildings and bridges) having supplemental passive systems (i.e. seismic fuses) to protect structures from excessive seismic demands (Celik and Bruneau 2011; Berman

2011; Walter Yang et al. 2010). To date, numerous types of metallic dampers have been developed and implemented in existing (for seismic retrofit purposes) and new buildings and bridges. Widely used energy dissipating metallic devices are added damping and stiffness (ADAS), triangular-plate added damping and stiffness (TADAS), steel plate shear walls (SPSWs), slit dampers, and BRBs (buckling restrained braces, a.k.a. unbonded braces) (Soong and Spencer 2002; Tsai et al. 1993; Berman et al. 2005; Chan and Albermani 2008; Wada et al. 1998; Sahoo et al. 2015a; Pandikkadavath and Sahoo 2016). Metallic dampers exhibit a robust hysteretic behavior for various deformation cases such as shear, flexure or combination of these as proposed by Sahoo et al. (2015b) and dissipate the seismic induced energy. BRBs of any kind have attracted much attention in terms of both theoretical and experimental research recently and have found many application possibilities as well (Takeuchi and Wada 2017). The very first experimental study about special devices which include U-shaped steel dampers (UDs) was conducted by Kelly et al. (1972). Currently, UDs have been widely accepted and implemented in buildings in Japan and other Asian countries. Suzuki et al. (2005) developed UD members as a component of base isolation system and reported that UD has stable hysteretic characteristics under

✉ Kurtulus Atasever
kurtulus.atasever@msgsu.edu.tr

Oguz C. Celik
celikoguz@itu.edu.tr

Ercan Yuksel
yukselerc@itu.edu.tr

¹ Department of Architecture, Mimar Sinan Fine Arts University (MSGSU), Meclis-i Mebusan Caddesi, No: 24, Findikli, 34427 Istanbul, Turkey

² Structural and Earthquake Engineering Division, Faculty of Architecture, Istanbul Technical University (ITU), Taskisla, Taksim, 34437 Istanbul, Turkey

³ Faculty of Civil Engineering, Istanbul Technical University (ITU), Maslak Campus, 34469 Istanbul, Turkey

different horizontal load directions. A minor effect of temperature between 20 and -10 °C was determined. Kato et al. (2005) presented that J-shaped steel dampers (a sort of U-damper) used under a spatial roof structure reduced story accelerations and shear effects. They also performed a parametric analysis to determine cyclic behavior of J-shaped damper (Kato and Kim 2006). Another configuration of UD is suggested by Tagawa and Gao (2012) where UD is inserted into a building frame together with a bracing member that exhibits tensile deformations only. Oh et al. (2012, 2013) carried out shake table tests to compare seismic responses of fixed base structure and base isolated structure that consists of laminated rubber bearings and slotted UDs made of high toughness and ordinary structural steels. These experimental results demonstrated that structural damage concentrated in UDs rather than other structural elements as per the design intent. Deng et al. (2013, 2015) carried out some experimental work to propose a UD called as the ‘crawler damper’ for bridges and optimize bidirectional behavior of UD with changing its shape considering dissipated energy and equivalent plastic strains. Special emphasis is paid to understand behavior under bidirectional loadings and fracture (or fatigue) life. Residual fracture life of UDs was investigated experimentally and analytically (Konishi et al. 2012; Kawamura et al. 2014) after the March 11th, 2011 Great East Japan (or Tohoku) Earthquake. They reported that fracture life curve fits well with the Manson-Coffin relation and significant fracture life remained after the earthquake. Jiao et al. (2014) carried out dynamic experiments to obtain hysteretic characteristic of UDs and proposed again Manson Coffin relation related to peak to peak shear angle. Ene et al. (2015) performed static and dynamic tests with bidirectional generated and realistic displacement orbit and proved that D_2 - J_f fatigue life model proposed by Kishiki et al. (2014) is accurate to predict the fatigue life of UDs. It is presented that unidirectional damage models are conservatively safe when compared to bidirectional damage models.

Even UDs could be designed with different shapes and materials (such as steel, aluminum, copper, etc.), the basic mechanism is to dissipate energy through large plastic deformation. When they are used in a base isolation system, such dampers are expected to work efficiently under different loading directions. Konishi et al. (2012) reported that UD has only used 5% of its expected fatigue life even under a $M_w = 9.0$ earthquake, showing that UDs were designed conservatively. Furthermore, in all cases considered to date, the idea of maximizing the dissipated energy by changing geometric properties of UDs for a given amount of material (e.g. the steel volume used) has not been investigated. The research presented here essentially aims to focus on this issue by developing and suggesting two various types of UDs incorporating circular perforations in the U-elements

and U-elements with nonparallel arms. Both unidirectional and bidirectional hysteretic behaviors of the developed dampers are obtained and compared with the existing damper configurations under the assumed cyclic displacement histories. The potential advantages such as more reasonable distribution of plasticity for the perforated dampers and better distribution of internal forces for the nonparallel arm dampers are discussed. The numerical results showed promise for use of such new configuration/modified dampers in new or seismic retrofit designs.

2 U-Damper Components and Possible Configurations

U-shaped steel dampers provide the seismic designer with stable hysteretic behavior, fatigue behavior, easy inspection, possible replacement following a major earthquake when needed, and less sensitivity to other secondary effects (i.e. temperature, frequency dependence). A typical UD has upper and lower base plates, shear studs welded to these plates, a selected number of U-elements, and sufficient number of fixing bolts to the upper and lower plates (Fig. 1a). They can be designed to meet the project specific features with various sizes, UD element numbers (e.g. 4, 6, 8 elements) and combinations (Fig. 1b). Numbers of U element to be used in an UD unit are depended on the seismic demand and locations of the columns in the building layout. Hysteretic behavior of the whole building is highly dependent on the hysteretic behavior of the UDs used. Also, analyzing a single UD in different directions is adequate to obtain the hysteretic behavior of an UD unit having several arms. As shown in Fig. 1c, hysteretic behavior of the UD unit with 4 single elements under 0° load can be obtained with the superimposed hysteretic curves of two UDs under 0° loading and the other perpendicular two UDs under the influence of 90° loading. Also, these dampers could be implemented in both reinforced concrete (RC) and steel framed buildings.

UDs can be used together with natural rubber bearings (NRBs) under building columns as shown in Fig. 2a or under girders without NRBs as shown in Fig. 2b to provide the building with almost the same hysteresis for any direction of seismic action by creating significant damping effect.

3 Proposed Damper Configurations

In this work, two different modifications are suggested in the existing UDs to possibly attain a better hysteretic behavior that would result in a fuller hysteretic curve and larger cumulative energy dissipation. A widely used solid (or unperforated) UD-S is taken as the reference damper as shown in Fig. 3a where the first and second heights of the

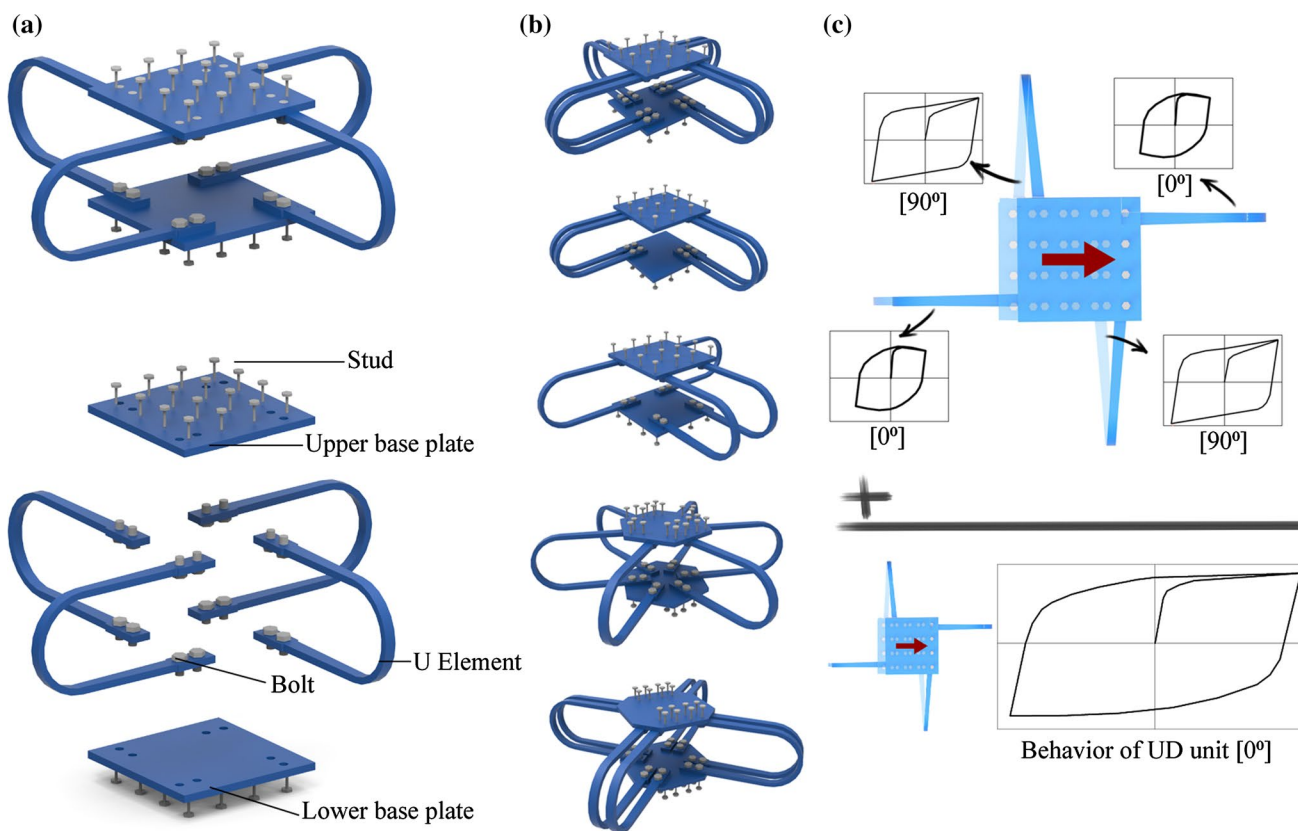


Fig. 1 Possible UD configurations **a** components of UD, **b** UDs with 4, 6, 8 arms and **c** hysteric curves of a single arm and at different loading directions and the superimposed hysteric curve for the whole device

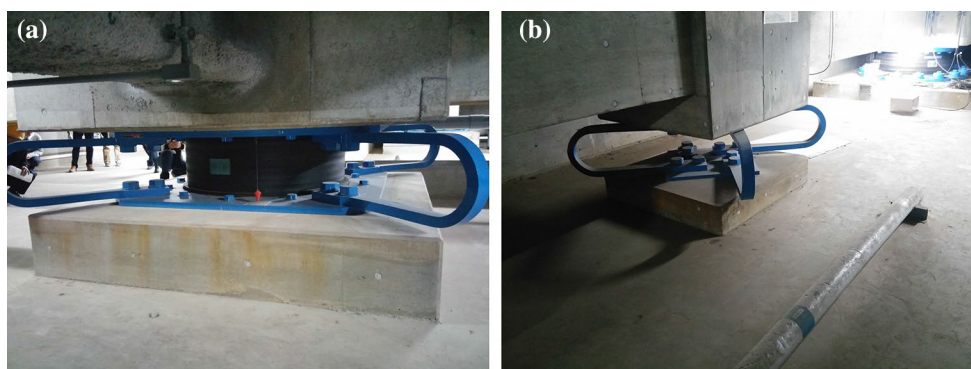


Fig. 2 Implementation of UDs in buildings **a** UDs with NRB, **b** UD without NRB (photo credit: Kurtulus Atasever)

damper H and H_2 are 175 mm, first and second widths w_1 and w_2 are respectively 45 and 60 mm, thickness of each arm t is 28 mm. The first type of damper uses evenly or unevenly spaced circular perforations in the U arms and named to be UD-P damper (Fig. 3b). It is obvious that circular holes become elliptic around the arc region of the arm after the bending process. In practice, an appropriate heat treatment can be applied to UDs during the bending of the steel plate. The main idea behind this modification with perforations

is to increase stress concentration near the circular holes and to have a more distributed plasticity along the whole length of the arm (not to concentrate strains at a point which is the case in regular UDs so far) in order to experience inelastic deformations in early stages of earthquake shaking. Here, the concept of stress concentration factor is crucial and Schulz (1942) calculated such factors for uniaxial tension with an infinite row of circular holes. According to this work, the maximum stress decreases when the holes get

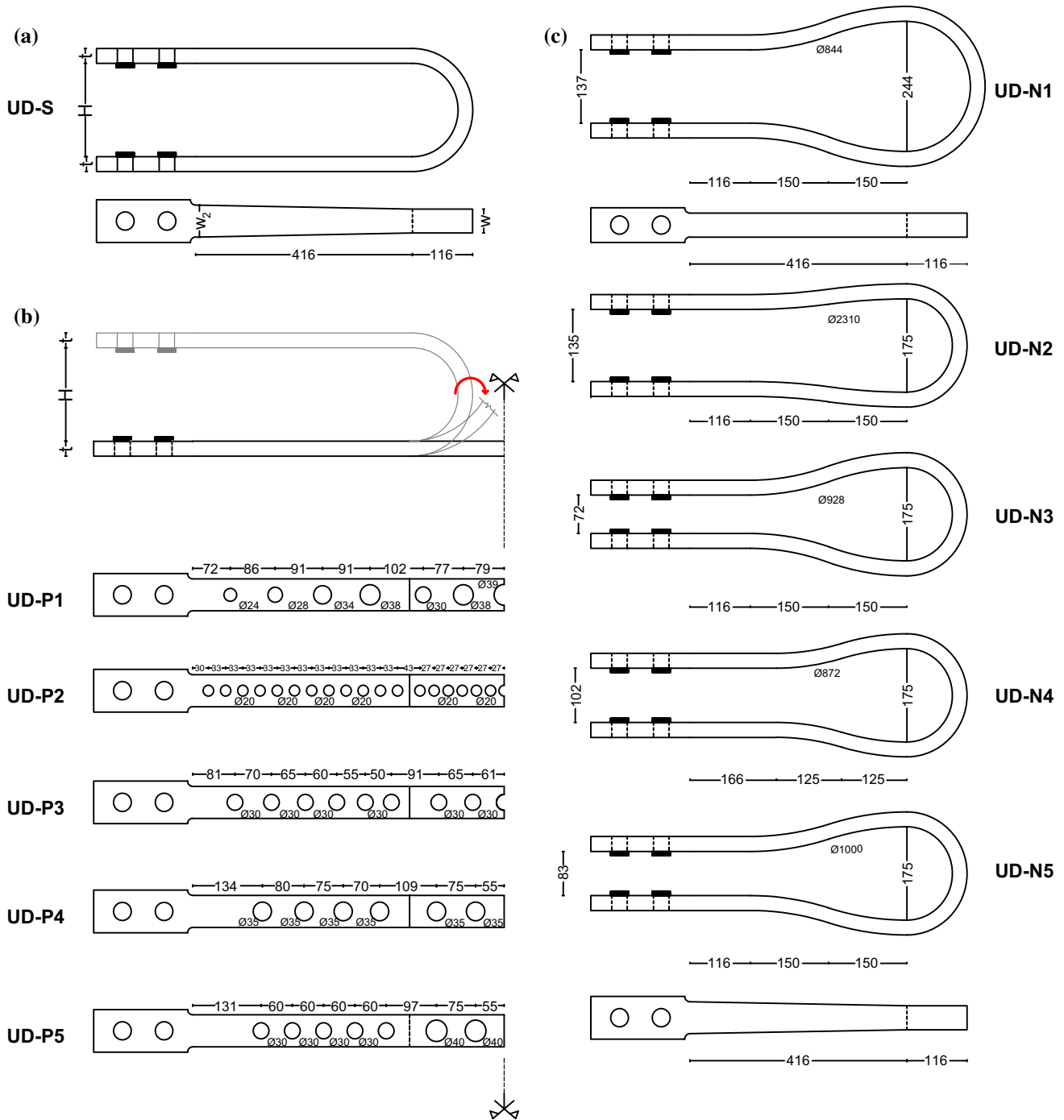


Fig. 3 Geometric properties of damper configurations a UD-S, b UD-P and c UD-N

closer to each other. However, in any case, stress concentration factor gets bigger values than one (i.e. 1.00) which means that increasing stress is satisfied with opening holes (Pilkey and Pilkey 2007).

The second type of UD is named as UD-N which is formed with bending the steel plates twice (Fig. 3c). In this case, the arms are not parallel anymore. As discussed

above, UDs have been widely used in a base isolation system with elastomeric bearings as additional damping element. Behavior of such an isolation system configuration is highly dependent on heights (H) of the UD and elastomeric bearing. Assuming a perfectly plastic behavior in steel parts, the maximum horizontal force P_{max} is basically obtained to be $P_{max} = \frac{\sigma_y w t^2}{2H}$ (Kelly et al. 1972) where σ_y , w , t are the yield

stress, width ($w = w_2$), and thickness respectively. According to this relation, the maximum force P_{\max} increases when H decreases (keeping other parameters as constant), which suggests that the height could be modified to attain higher lateral force capacities when needed. In other words, a better internal force distribution could be obtained by using other geometrical shapes. To address this, the designed UD-N type damper contains two heights (H and H_2) to control cyclic behavior. Because of the iterative design process of seismic isolated structure (pre-design, design, performance analysis after design), it is highly important having alternative shapes to obtain the desired behavior. For comparison purposes, developed dampers of five different hole configurations (namely UD-P1, UD-P2, UD-P3, UD-P4, and UD-P5) and five different non-parallel arm configurations (namely UD-N1, UD-N2, UD-N3, UD-N4, UD-N5) are considered in this work. The design criterion was to provide equal cross section areas for parts of UD. Total volume (or mass) of steel used was set to be equal to each other for making a fair performance comparison possible.

4 3D Numerical Modeling

4.1 Displacement Histories

In order to simulate hysteretic behavior of UDs under lateral loads, a 3D finite element model (FEM) is developed with ABAQUS 6.14. UDs are designed not to have plastic deformations around connection parts such as bolts, steel plates, and heads of damper. Since these parts are sufficiently stiff to remain elastic under loading, only arms and curved part of a damper are considered in the finite element (FE) model as illustrated in Fig. 4. Furthermore, cross section of the lower head is assumed to be fixed. Cyclic displacements are applied with the help of a reference point (RP) which is coupled to section of upper head to move together in all degrees of freedom. After many trial numerical analyses, size of the finite element is selected to be 10 mm and thickness of UD divided into four elements where the element type is chosen as 3D8R (8-node brick element, reduced integration, hourglass control). All analyses are carried out with a computer having i7-4770 CPU, 3.40 GHz, 3401 MHz, 4 Core, 8 logical processors, and 8.00 GB installed physical memory (RAM).

Two different loading protocols are used for this study. First, a sine wave loading protocol (Fig. 5a) is used to mostly determine mechanical characteristics of energy dissipating devices. The sine wave is defined as $y(t) = A \sin(\omega t + \varphi)$ where A , ω , φ are the amplitude, angular frequency, and lag phases respectively. In this relation A , ω , φ are chosen as 250, $\pi/2$ rad/s, and 0 as same as in an experimental study made by Jiao et al. (2015).

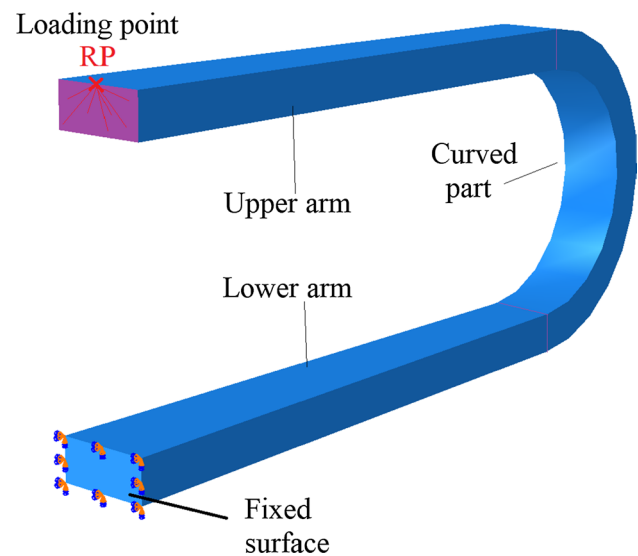


Fig. 4 Finite element model of UD and boundary conditions

In Type A loading, the numerical analysis is performed for 30 cycles. Type B loading protocol which considers lateral displacement of structure under extreme earthquakes, is used to compare the new UD designs with the existing damper types. This protocol has been used by Suzuki et al. (2005) to determine mechanical properties of a selected type of UD. Loading velocity is selected to be 10 mm/s and amplitude of each of seven cycle is 10, 15, 25, 50, 100, 200 and 300 mm respectively (Fig. 5b).

4.2 Material Model

One of the most important issue in FE modeling is to create an appropriate material model to capture/simulate the real behavior. In this work, a combined nonlinear isotropic and kinematic hardening model is selected to obtain steel behavior subjected to cyclic loadings. The hardening model was produced by Armstrong and Frederick (1966) and modified by Lemaître and Chaboche (1990). This model consists of isotropic and kinematic hardening components. Isotropic hardening is defined as a model having a growing yield surface depending upon increasing of stress without leaving its origin (Fig. 6a). Radius of yield surface of isotropic hardening component is given in Eq. (1)

$$\sigma^0 = \sigma|_0 + Q_\infty (1 - \exp(-b\bar{\epsilon}^{pl})) \quad (1)$$

where σ^0 is radius of the yield surface, $\sigma|_0$ is initial yield surface size, Q_∞ and b represent material parameters which are derived from experimental studies. $\bar{\epsilon}^{pl}$ is defined as the equivalent plastic strain. Kinematic hardening is a moving yield surface as a rigid body without expanding regarding increase of stress. This hardening component is required to

Fig. 5 Loading protocols **a** Type A and **b** Type B

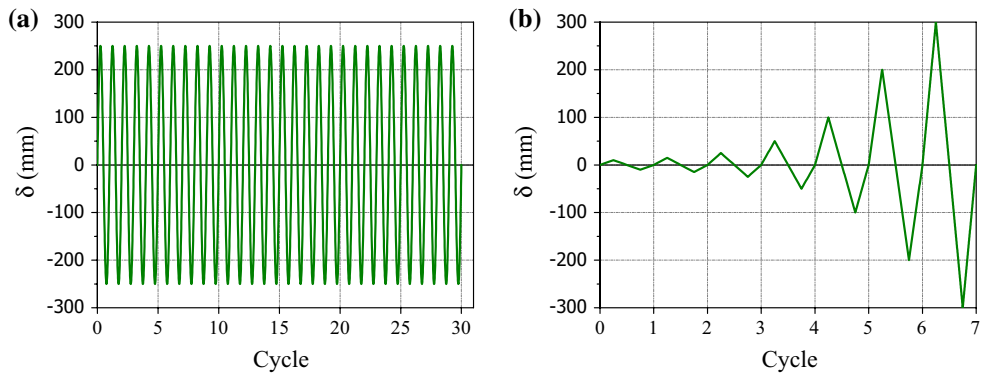


Fig. 6 Hardening models: **a** isotropic hardening, **b** kinematic hardening and **c** combined hardening. Adopted from Jirásek and Bazant (2002)

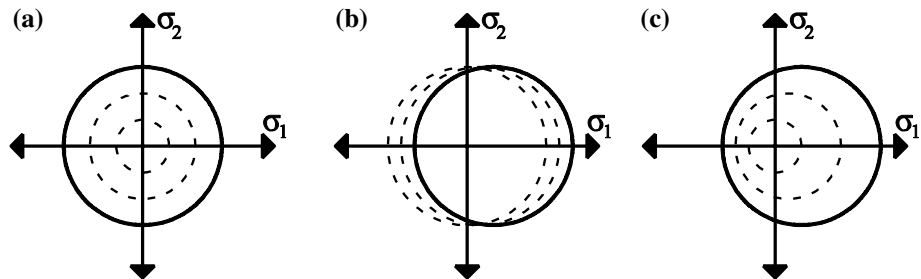


Table 1 Material parameters

| Material | C_k (MPa) | γ_k | Q_∞ (MPa) | b | σ_0 (MPa) |
|----------|-------------|------------|------------------|-----|------------------|
| SN490B | 5792 | 28 | 207 | 4 | 310 |

model the Bauschinger effect which is observed in metals subjected to cyclic loading (Fig. 6b) (e.g. Bruneau et al. 2011) Movement of the yield surface center can be obtained with Eq. (2)

$$\dot{\alpha}_k = C_k \frac{1}{\sigma_0} (\sigma - \alpha) \dot{\epsilon}^{pl} - \gamma_k \alpha_k \dot{\epsilon}^{pl} \tag{2}$$

where α back stress tensor, $\dot{\epsilon}^{pl}$ incremental change in equivalent plastic strain, α_k incremental change in the back stress tensor, γ_k and C are material parameters. Overall back stress can be defined as given in Eq. (3)

$$\alpha = \sum_{k=1}^N \alpha_k \tag{3}$$

Figure 6c reveals that the combined hardening model is the sum of isotropic and kinematic hardening models. In other words, not only expands the size of yield surface but also location of yield surface moves. SN490B steel type is used in this work. The hardening parameters depicted in Table 1 are used to verify the proposed FE model and to obtain hysteretic behavior of new UD designs. These

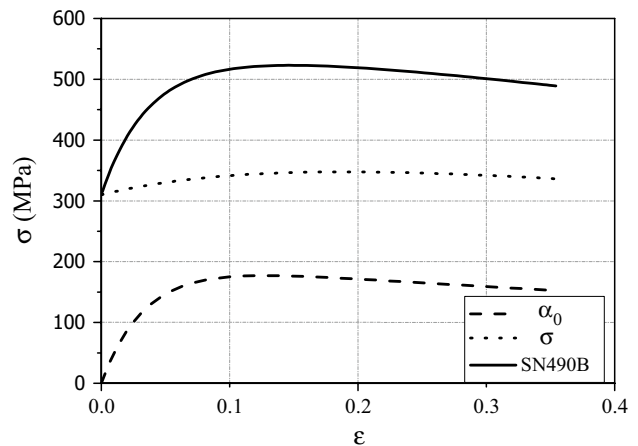


Fig. 7 SN490B material model

parameters are obtained from a comprehensive study of Myers et al. (2009). One-dimensional representation of combined hardening model is shown in Fig. 7 where σ^0 and α represent isotropic and kinematic hardening of material model respectively.

From uniaxial test results on this steel, Myers et al. (2009) found that the yield and ultimate (tension) stresses were 345 MPa and is 524 MPa respectively. However, in an experimental study which is used to verify the developed FE model, the calculated (i.e. engineering stresses) yield and ultimate stresses are obtained to be 378 and 544 MPa respectively. Because of acceptable differences of the results, hardening parameters are used exactly as the proposed values

of Myers et al. (2009). However, this difference is taken into consideration while evaluating the obtained hysteretic curves in the forthcoming sections. Note that, as explained before, fracture is not modeled in this work for the reason that UD's have significant fatigue/fracture life as proved in the last major earthquakes.

5 Analysis Results

5.1 Verification of the Model

The first analysis was conducted to verify the numerical model developed in this work on a conventional UD (UD40) that was experimentally studied by Suzuki et al. (1999). As shown in Fig. 8, the FE model developed in this work is sufficient to represent the lower bound of the hysteretic curve for 0° loading direction. However, representation of isotropic hardening of the yield surface is somewhat limited. This is attributed to the difference between the material model followed and coupon test behavior as mentioned earlier. Since general shapes of the hysteretic curves from experimental and numerical analyses are in good agreement, the hardening parameters have not been calibrated. A more detailed information about this comparison can be found in Atasever et al. (2017).

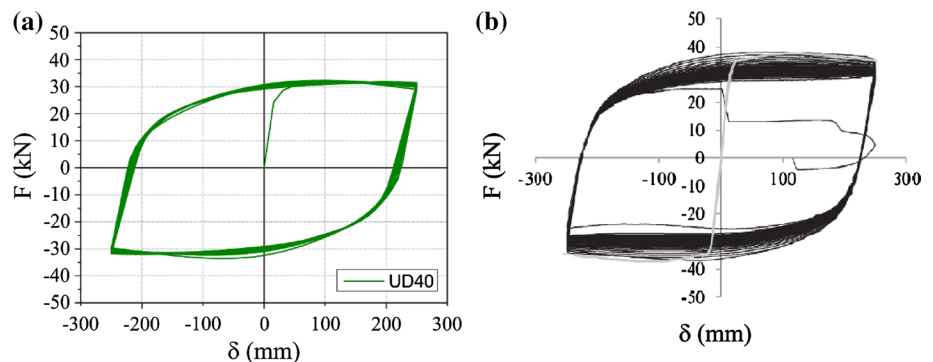
5.2 Behavior of Proposed Damper Configurations

After verification of the FE model with an acceptable accuracy, numerical analyses conducted for newly designed dampers with holes and nonparallel arms and analysis results are presented graphically in Fig. 9. Amount of dissipated energy (E_p) which is calculated by the sum of area below a hysteretic curve is the first criterion for evaluating seismic performances of metallic dampers. Except UD-N1, all UD-N type dampers have larger hysteretic area than UD-S. UD-N3 dissipated the most cumulative energy (79.3 kNm) after 7 cycles. UD-P type dampers have lower amount of dissipated energy than UD-S dampers. UD-P2

has the highest amount of dissipated energy (55.5 kN m) which is 87% of UD-S. Effective stiffness (k_{eff}) is the ratio of sum of absolute values of minimum and maximum reaction forces to sum of absolute values of minimum and maximum displacements for each cycle. This parameter is significant to understand the behavior of UD under minor and extreme loads. Effective stiffness at last cycle (at 300 mm) around 5% of the first effective stiffness (at 10 mm) for all dampers. Reaction force at maximum displacement for each cycle ($F-\delta_{\text{max}}$) is a key parameter for designing process. According to results obtained from this numerical study, maximum reaction forces occur at 100 and 200 mm displacement levels. Strength degradations at the last displacement cycle are 13% for UD-S, 8% for UD-P1, and 4% for UD-N3. These results show that all dampers have stable hysteretic behavior even at highest displacement (300 mm) levels. Another crucial parameter is effective damping ratio (ξ_{eff}) which represents dissipated energy in terms of equivalent viscous damping. Based on the cumulative hysteretic responses under the selected loading histories, except for UD-P1, all UD-P type dampers have barely higher effective damping ratios than UD-S ($\xi_{\text{eff}} = 56\%$). With a minimum effective damping ratio of 52% at the maximum displacement, it can be said that the developed/improved UD's in different geometries dissipate significant hysteretic energy and therefore have sufficient ξ_{eff} values for seismic application purposes.

A further study is performed to trace the deflected shapes and plastified locations of an U-shaped damper element. For this purpose, stress distributions at 50, 100, 150, 200, 250, and 300 mm lateral displacement (δ^+) values are given in Fig. 10 for the last cycles of loading Type B. As shown in Fig. 10, UD-S reaches high stresses after 100 mm displacement while UD-N1 gets high values after 250 mm lateral displacement. When compared to UD-S, UD-N1 possesses lower but concentrated stresses resulting from the modified geometry. For UD-P1, as per design target, stresses are concentrated around the holes, causing larger plastic deformations. Because UD-P1 reaches high stress values even at 50 mm lateral displacement, yielding of the damper starts

Fig. 8 Hysteretic behaviors for 0° loading **a** FE analysis result; **b** experimental result. Reproduced with permission from Jiao et al. (2015)



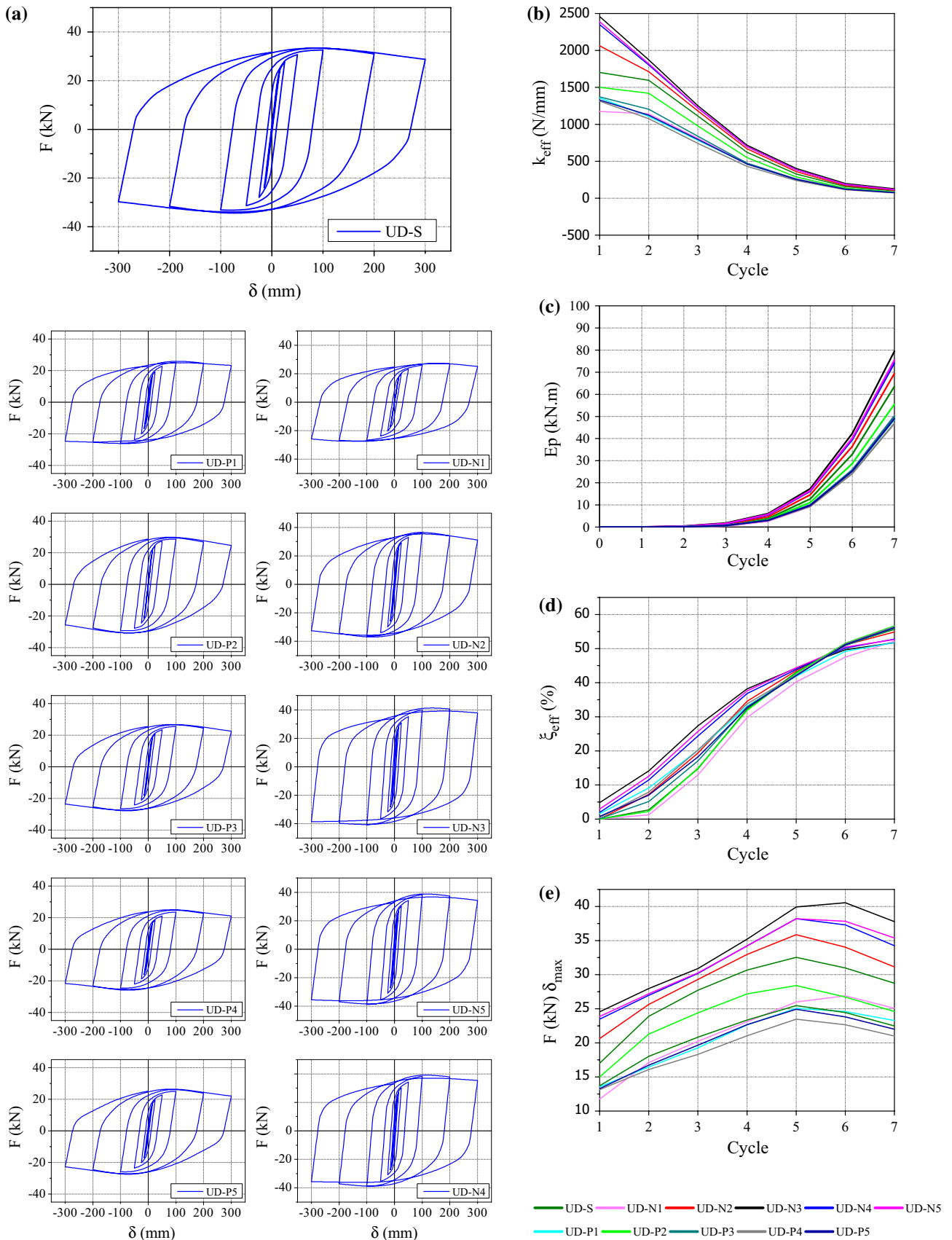


Fig. 9 a Hysteretic curves of UD-S, UD-P and UD-N, b effective stiffness, c dissipated hysteretic energy, d effective damping and e force at maximum displacement



Fig. 10 Stress distributions and deformed shapes under 0° loading a UD-S, b UD-N1 and c UD-P1

at early stages of displacements, which could be useful in seismic applications.

5.3 Effect of Bidirectional Loading

Design of seismically isolated structures is an iterative procedure which starts with preliminary design to verification of the design. In the last step of design procedures, it is expected to perform detailed 3 dimensional (3D) analyses which take into account 2 or 3 dimensional strong ground motion effects. Thus, to show the behavioral differences, this part of study involves the behavior of UD under bidirectional loading. As a numerical example, following the modeling procedure given in previous sections, a unit damper which consists of 4 single UD-N2 in each orthogonal directions is numerically investigated under 0° , 45° , and 90° loading direction as shown in Fig. 11a.

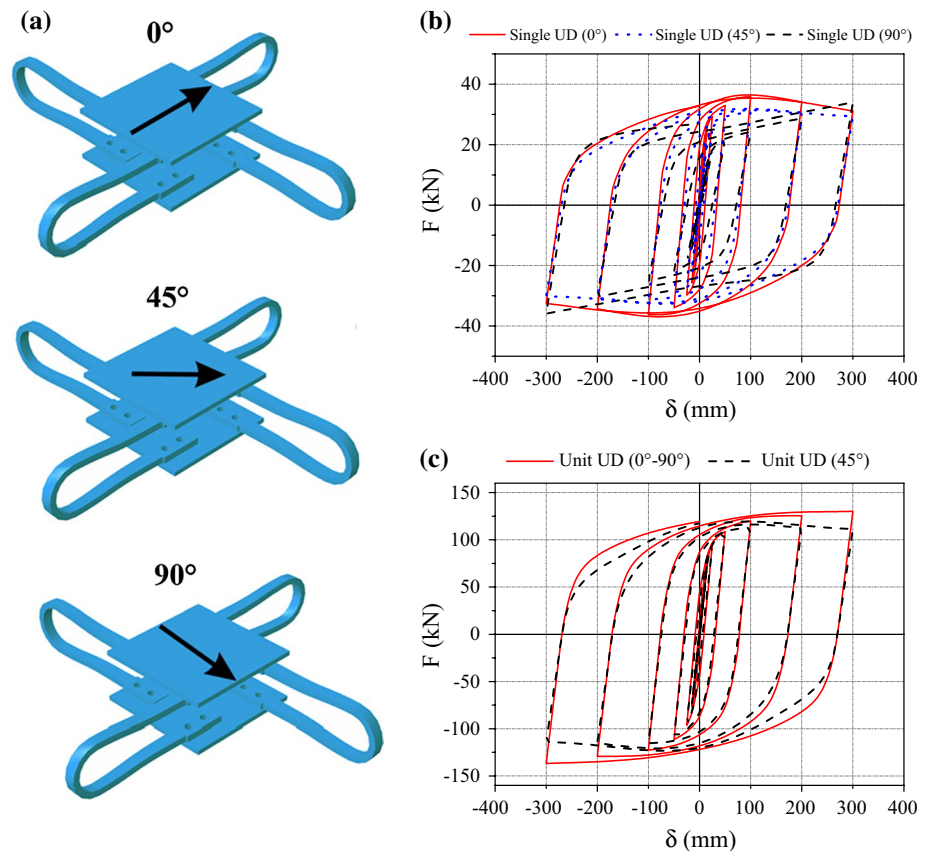
As explained in Fig. 1, when the unit damper is subjected to 0° or 90° loading, two single UDs are subjected to 0° loading and the other two are subjected to 90° loading. In the case where unit damper is under 45° loading, all four single UDs are under 45° loading. Therefore, firstly hysteretic behaviors of a single UD under 0° , 45° , and 90° loading directions should be obtained (Fig. 11b). Increasing the angle of loading directions until 90° leads to a decrease in

the dissipated energy since hysteretic curves under 0° loading is fuller than 45° and 90° loading directions. Although reaction forces and stiffnesses differ from each other, these parameters are nearly the same at maximum displacements which represent a stable behavior. The different behaviors of single UD under different loading directions could be eliminated by using symmetric unit dampers. As shown in Fig. 11c, despite there is a little strength degradation at the last cycle of displacements, hysteretic behaviors of a unit damper under 0° , 45° and 90° loading is very similar which is desirable in seismic design and retrofit applications. While cumulative plastic energy dissipation difference between 0° and 90° loading directions for a single UD under Type B loading protocol is as high as 33%, this difference is 0% for unit damper composed of 4UN-N2.

As shown in Fig. 12, stress concentration regions also differ when loading direction changes. Stresses are higher at middle of upper and lower arm of UD. However, when the loading angle increases, highly stressed locations get closer to the end of upper and lower arms. Stresses are more concentrated under 90° loading but starts lately (at 200 mm) to get higher values than under 0° loading. This results in lower dissipated energies.

To evaluate performance of different UD configurations, yield displacement (δ_Y), equivalent plastic strain at last step

Fig. 11 Unit UD (4UD-N2) consisted of 4 single UD-N2 under **a** 0° , 45° , 90° loading directions and hysteretic behaviors, **b** for single and **c** for unit UD



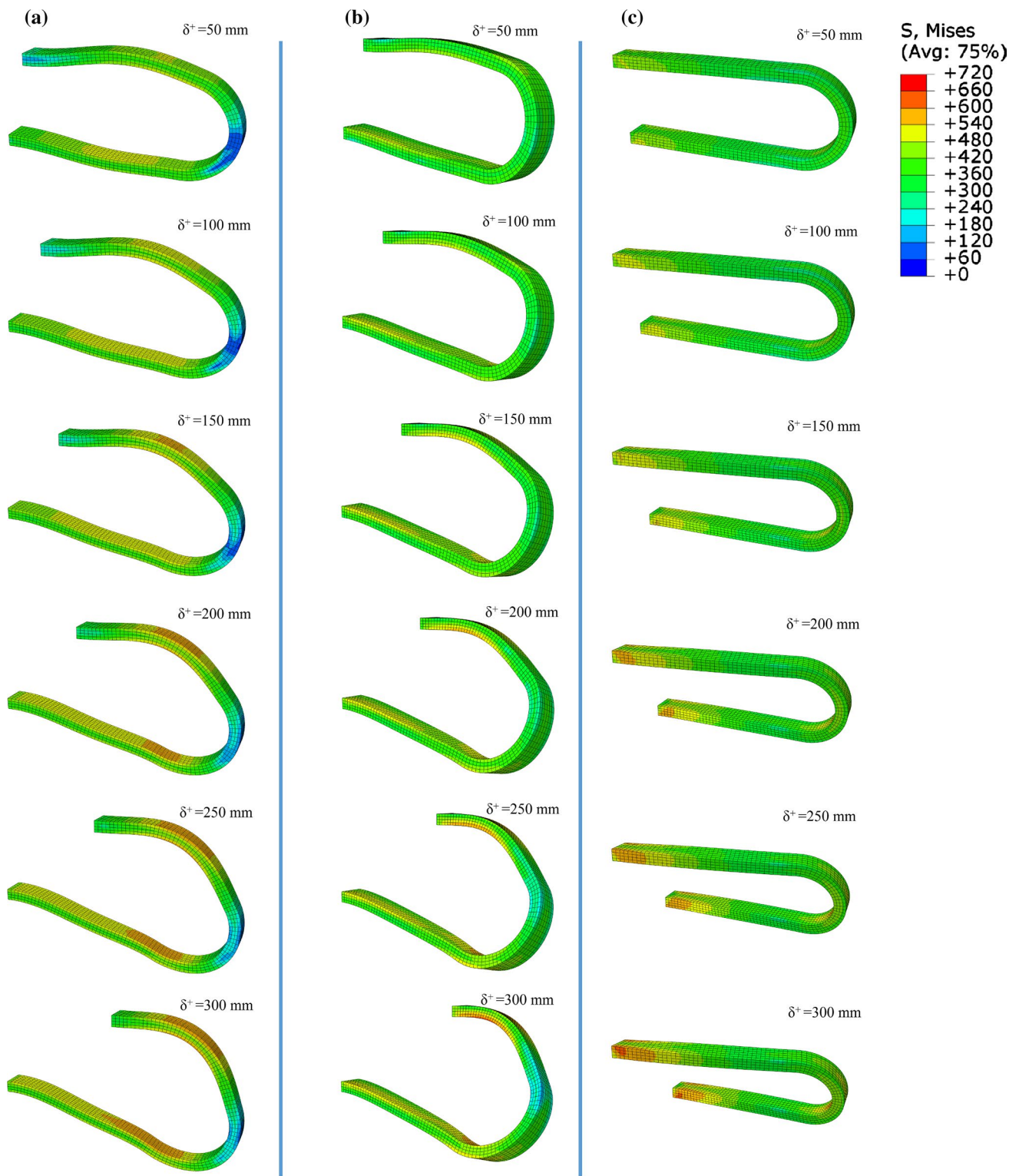
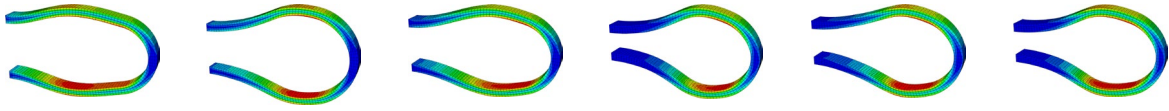
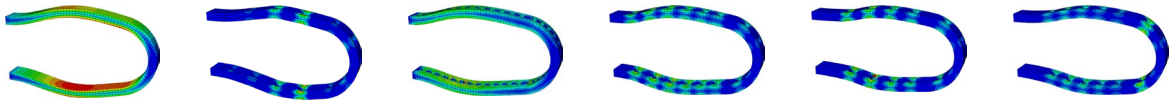


Fig. 12 Stress distributions and deformed shapes of UD-S at different displacements (δ) under **a** 0° , **b** 45° and **c** 90° loading directions

($PEEQ_L$), ratio of the first effective stiffness to first effective stiffness of UD-S (K^{1st}/K_{UD-S}^{1st}), ratio of cumulative dissipated energy to cumulative dissipated energy of UD-S

(E_p/E_{pUD-S}), effective damping ratio at first cycle (ξ_1), and concentration of plastic deformation at last step of finite element analysis are given in Table 2. Height of damper is the

Table 2 Comparison behavioral values of different UD configurations

| | UD-S | UD-N1 | UD-N2 | UD-N3 | UD-N4 | UD-N5 |
|--|------|-------|-------|-------|-------|-------|
| δ_Y (mm) | 12.5 | 15 | 10 | 7.5 | 10 | 10 |
| PEEQ _L | 0.27 | 0.28 | 0.35 | 0.5 | 0.43 | 0.43 |
|  | | | | | | |
| K^{1st}/K_{UD-S}^{1st} | 1 | 0.69 | 1.21 | 1.45 | 1.38 | 1.4 |
| E_p/E_{pUD-S} | 1 | 0.79 | 1.09 | 1.25 | 1.17 | 1.19 |
| ξ_1 (%) | 0 | 0 | 0 | 5 | 2 | 3 |
| | UD-S | UD-P1 | UD-P2 | UD-P3 | UD-P4 | UD-P5 |
| δ_Y (mm) | 12.5 | 7.5 | 10 | 10 | 10 | 7.5 |
| PEEQ _L | 0.27 | 1.66 | 0.43 | 0.74 | 1.06 | 1.17 |
|  | | | | | | |
| K^{1st}/K_{UD-S}^{1st} | 1 | 0.8 | 0.88 | 0.81 | 0.77 | 0.78 |
| E_p/E_{pUD-S} | 1 | 0.77 | 0.87 | 0.79 | 0.74 | 0.77 |
| ξ_1 (%) | 0 | 2 | 0 | 0 | 0 | 1 |

most effective factor on hysteretic behavior of UD. Results show that only UD-N1 has lower first effective stiffness than UD-S, while in other UD-Ns (i.e. UD-N2, UD-N3, UD-N4, UD-N5) type of dampers, E_p and K_{1st} increased inversely proportional to decreasing the height of damper. Increasing first effective stiffness provides more reaction forces and yielding of steel at early stages of displacement, thus damping becomes effective at first/early cycles of the loading that could be preferred in some seismic design applications.

Plastic deformations of UD-P1 do not well distribute along the damper and concentrated on biggest holes at upper and lower arms instead. This is attributed to the selected relatively large size of holes ($d/t = 1.39$) that have negatively affected the behavior of damper. UD-P2 which has uniform hole configuration has resulted in more distributed plastic deformations near the holes. Increasing hole radius in UD-P3 and UD-P4 has led to more concentrated stresses near the holes on upper and lower arms. This resulted in that curved part of UD has minor contribution on the plastic mechanism. Plastic deformations of UD-P5 are concentrated near the holes on the curved part.

6 Conclusions

The following major conclusions can be drawn from this numerical study performed on developed UDs having various geometries:

1. Unlike the conventional UD (i.e. solid and parallel armed), two (UD-P with holes and UD-N with non-parallel arms), new UDs configurations are developed and their performances are numerically compared. The behavioral parameters obtained from hysteretic curves are discussed.
2. All dampers have more than 50% ($\xi_{eff} = 0.50$) damping ratios at large deformations, proving that the newly developed dampers dissipate significant amount of energy.
3. Based on the same material volume criterion, UD-P has lower first effective stiffness, and UD-N dissipates more energy at the same cycle. This shows that both damper types have merit in use of seismic applications and that the selection of the damper configuration is dependent on the design specific issues.
4. Hole sizes play an important role on the hysteretic behavior. In UD-P1 and UD-P2, plastic deformations concentrated around the biggest hole, and thus hysteretic behavior of the damper is governed by the weakest zone. Based on the available data used in this numerical work, it seems that the hole diameter-to-thickness ratio should be smaller (e.g. $d/t < 0.71$) and distributed equally on the damper since this configuration would provide the designer with more distributed plastic deformations and a better seismic response.
5. Hysteretic behavior of the U-shaped dampers is also investigated under bidirectional loading conditions. Numerical analyses on the selected damper configura-

tions and loading angles demonstrate that the behavioral parameters such as strength, stiffness, and dissipated energy do not change much when symmetrical configurations are used as damper units.

References

- Armstrong, P. J., & Frederick, C. O. (1966). *A mathematical representation of the multiaxial Bauschinger effect*. Central Electricity Generating Board [and] Berkeley Nuclear Laboratories, Research and Development Department.
- Atasever, K., Celik, O. C., & Yuksel, E. (2017). Modelling hysteretic behaviour of U-shaped steel dampers. *Ce/Papers*, 1(2–3), 3239–3248.
- Berman, J. W. (2011). Seismic behavior of code designed steel plate shear walls. *Engineering Structures*, 33(1), 230–244.
- Berman, J. W., Celik, O. C., & Bruneau, M. (2005). Comparing hysteretic behavior of light-gauge steel plate shear walls and braced frames. *Engineering Structures*, 27(3), 475–485.
- Bruneau, M., Uang, C.-M., & Sabell, R. (2011). *Ductile design of steel structures* (2nd ed.). New York: McGraw-Hill Professional.
- Celik, O. C., & Bruneau, M. (2011). Skewed slab-on-girder steel bridge superstructures with bidirectional-ductile end diaphragms. *Journal of Bridge Engineering*, 16(2), 207–218.
- Chan, R. W. K., & Albermani, F. (2008). Experimental study of steel slit damper for passive energy dissipation. *Engineering Structures*, 30(4), 1058–1066.
- Deng, K., Pan, P., Su, Y., & Xue, Y. (2015). Shape optimization of U-shaped damper for improving its bi-directional performance under cyclic loading. *Engineering Structures*, 93(2015), 27–35.
- Deng, K., Pan, P., & Wang, C. (2013). Development of crawler steel damper for bridges. *Journal of Constructional Steel Research*, 85, 140–150.
- Ene, D., Kishiki, S., Yamada, S., Jiao, Y., Konishi, Y., Terashima, M., et al. (2015). Experimental study on the bidirectional inelastic deformation capacity of U-shaped steel dampers for seismic isolated buildings. *Earthquake Engineering and Structural Dynamics*, 45(2), 173–192.
- Jiao, Y., Kishiki, S., Ene, D., Yamada, S., Kawamura, N., & Konishi, Y. (2014). Plastic deformation capacity and hysteretic behaviour of U-shaped steel dampers for seismic isolated buildings under dynamic cyclic loadings. In *Tenth U.S. National Conference on Earthquake Engineering*. Alaska.
- Jiao, Y., Kishiki, S., Yamada, S., Ene, D., Konishi, Y., Hoashi, Y., et al. (2015). Low cyclic fatigue and hysteretic behavior of U-shaped steel dampers for seismically isolated buildings under dynamic cyclic loadings. *Earthquake Engineering and Structural Dynamics*, 44(10), 1523–1538.
- Jirásek, M., & Bazant, Z. (2002). *Inelastic analysis of structures*. West Sussex: Wiley.
- Kato, S., & Kim, Y. B. (2006). A finite element parametric study on the mechanical properties of J-shaped steel hysteresis devices. *Journal of Constructional Steel Research*, 62(8), 802–811.
- Kato, S., Kim, Y.-B., Nakazawa, S., & Ohya, T. (2005). Simulation of the cyclic behavior of J-shaped steel hysteresis devices and study on the efficiency for reducing earthquake responses of space structures. *Journal of Constructional Steel Research*, 61(10), 1457–1473.
- Kawamura, N., Konishi, Y., Terashima, M., Jiao, Y., Ene, D., Kishiki, S., & Yamada, S. (2014). Evaluation methods of residual fatigue life of U shaped steel dampers after extreme earthquake excitation. In *Tenth U.S. National Conference on Earthquake Engineering*. Alaska.
- Kelly, J., Skinner, R., & Heine, A. (1972). Mechanism of energy absorption in special devices for use in earthquakes resistant structures. *Bulletin of the New Zealand National Society for Earthquake Engineering*, 5(3), 63–88.
- Kishiki, S., Yamada, S., Ene, D., Konishi, Y., Kawamura, N., & Terashima, M. (2014). Evaluation of plastic deformation capacity of U shaped steel dampers for base-isolated structures under 2D horizontal loading. In *Tenth U.S. National Conference on Earthquake Engineering*. Alaska.
- Konishi, Y., Kawamura, N., Terashima, M., Kishiki, S., Yamada, S., Aiken, I., Black, C., Murakami, K., & Someya, T. (2012). Evaluation of the fatigue life and behavior characteristics of U-shaped steel dampers after extreme earthquake loading. In *15th World Conference on Earthquake Engineering*. Lisbon, Portugal.
- Lemaître, J., & Chaboche, J.-L. (1990). *Mechanics of solid materials*. Cambridge: Cambridge University Press.
- Myers, A. T., Deierlein, G. G., & Kanvinde, A. (2009). *Testing and probabilistic simulation of ductile fracture initiation in structural steel components and weldments*. Stanford: Stanford University.
- Oh, S.-H., Song, S.-H., Lee, S.-H., & Kim, H.-J. (2012). Seismic response of base isolating systems with U-shaped hysteretic dampers. *International Journal of Steel Structures*, 12(2), 285–298.
- Oh, S., Song, S., Lee, S., & Kim, H. (2013). Experimental study of seismic performance of base-isolated frames with U-shaped hysteretic energy-dissipating devices. *Engineering Structures*, 56(2013), 2014–2027.
- Pandikkadavath, M. S., & Sahoo, D. R. (2016). Analytical investigation on cyclic response of buckling-restrained braces with short yielding core segments. *International Journal of Steel Structures*, 16(4), 1273–1285.
- Pilkey, W. D., & Pilkey, D. F. (2007). *Peterson's stress concentration factors*. Hoboken, NJ: Wiley.
- Sahoo, D. R., Sidhu, B. S., & Kumar, A. (2015a). Behavior of unstiffened steel plate shear wall with simple beam-to-column connections and flexible boundary elements. *International Journal of Steel Structures*, 15(1), 75–87.
- Sahoo, D. R., Singhal, T., Taraitia, S. S., & Saini, A. (2015b). Cyclic behavior of shear-and-flexural yielding metallic dampers. *Journal of Constructional Steel Research*, 114, 247–257.
- Schulz, K. J. (1942). On the state of stress in perforated strips and plates. In *Proceedings of the Koninklijke Nederlandse Akademie van Wetenschappen*, Amsterdam.
- Soong, T. T., & Spencer, B. F. (2002). Supplemental energy dissipation: State-of-the-art and state-of-the-practice. *Engineering Structures*, 24(3), 243–259.
- Suzuki, K., Saeki, E., & Watanabe, A. (1999). Experimental study of U-shaped steel damper. Part 1: Test of single U-shaped damper. Part 2: Test of U-shaped dampers with rubber bearings. In *Proceedings of Architectural Institute of Japan (AIJ) Annual Conference, B-2* (pp. 665–668).
- Suzuki, K., Watanabe, A., & Saeki, E. (2005). *Development of U-shaped steel damper for seismic isolation system*. Nippon Steel Technical Report.
- Tagawa, H., & Gao, J. (2012). Evaluation of vibration control system with U-dampers based on quasi-linear motion mechanism. *Journal of Constructional Steel Research*, 70(2012), 213–225.
- Takeuchi, T., & Wada, A. (2017). *Buckling-restrained braces and applications*. The Japan Society of Seismic Isolation (JSSI).
- Tsai, K.-C., Chen, H.-W., Hong, C.-P., & Su, Y.-F. (1993). Design of steel triangular plate energy absorbers for seismic-resistant construction. *Earthquake Spectra*, 9(3), 505–528.
- Wada, A., Saeki, E., Takeuchi, T., & Watanabe, A. (1998). Development of unbonded brace. *Nippon Steel's Unbonded Braces (promotional document)* (pp. 1–16).
- Walter Yang, C.-S., DesRoches, R., & Leon, R. T. (2010). Design and analysis of braced frames with shape memory alloy and energy-absorbing hybrid devices. *Engineering Structures*, 32(2), 498–507.